Predicting muscle forces in the shoulder by constraining the inverse optimisation with EMG and a forward muscle model

Bart Bolsterlee, TU Delft, Faculty of 3mE, Biomedical Engineering

Abstract

The Dutch Shoulder and Elbow Model (DSEM) is a musculoskeletal model of the shoulder that can be used to predict internal shoulder loading (muscle forces, joint reaction forces, etc.). The DSEM uses an inverse optimisation method to predict muscle forces from net joint moments. In this study two new modes are presented that constrain the inverse optimisation with muscle force boundaries based on muscle dynamics (inverse forward dynamical mode) and boundaries based on EMG-recordings (EMG-assisted mode). The new modes were validated with measurements of two standardised movements (abduction and anteflexion) from two subjects. A proof of concept has been given that both new modes work. It was concluded that DSEM predictions can be dominated by morphological differences between the subject and the cadaver on which the DSEM is based. Until better scaling routines are developed the IFDO mode is not very useful. When EMG-constraints are added, muscle and GH-joint reaction forces are predicted to be higher. Adding EMG for one muscle can predict cocontraction in other muscles. By adding EMG-based constraints, the DSEM can account for individual strategies in control strategy for the data that was analysed and is therefore an interesting topic for future research.

1. Introduction

For clinical purposes and for basic understanding of how the nervous system controls movement of the limbs for both healthy and pathological people, the biomechanist is interested in the relationship between external loading (external forces and accelerations) and internal loading (joint moments, ligament and muscle forces, joint reaction forces, etc.) on the human body. Because it is very difficult to measure internal loading *in vivo*, models are used. A *musculoskeletal* model describes the relationship between movements of the skeleton, joint moments and muscle forces and is a useful tool for estimating mechanical loading on the human musculoskeletal system. Musculoskeletal models are used for a variety of goals, most importantly they

- provide insight into human function (eg. coordination, muscle function, energy usage),
- allow for analysis of clinical problems (eg. diagnosis, improvement and development of treatments, development of prostheses),
- can be used to predict the response of the body to an intervention in the musculoskeletal system (eg. the effect of tendon transfer [16]).

For the shoulder musculoskeletal models of different complexity are used [6, 12, 13, 17]. Some models do not include scapular motion, but this would be an oversimplification for higher humeral elevation angles. Thorax, clavicle and scapula are connected via the sternoclavicular joint and acromioclavicular joint. On the dorsal side the medial border of the scapula moves over the thoracic surface on the scapulothoracic gliding plane, turning the shoulder girdle into a closed-chain mechanism. The Dutch Shoulder and Elbow Model [20, 21] is a musculoskeletal model of the shoulder and is the model that is used in this study to predict individual muscle forces with.

The inverse mode of the DSEM (see 1.3) does not use muscle dynamics (force-length-velocity relationship) for its prediction of muscle forces. In this study a new mode is presented that narrows the solution space of the inverse optimisation by putting boundaries on muscle forces based on muscle dynamics.

In its current form, the inverse DSEM can not account for individual differences in control strategy of muscle recruitment. To include individual strategies, also a mode that further constrains the inverse DSEM with electromyographic (EMG) recordings is presented. Evaluation of the new modes is based on measurements of two standardised movements (anteflexion and abduction) at different speeds.

1.1. Dutch Shoulder and Elbow Model

The DSEM is a large-scale finite-element musculoskeletal model of the shoulder and elbow, consisting of six bones (humerus, clavicle, scapula, thorax, radius and ulnar), five joints (glenohumeral (GH), acromioclavicular (AC), sternoclavicular (SC), humeroulnar (HU) and radioulnar (RU) joint), a scapulothoracic gliding plane and all 31 muscles (divided into 139 muscle elements [23]) and extracapsular

ligaments crossing these joints. The number of degrees of freedom (17), bones, muscles and ligaments makes the DSEM one of the most detailed mechanical shoulder models. Input to the inverse DSEM is formed by time series of cardan angles of bone rotations and external forces. Output are net joint moments, joint reaction forces and forces, lengths and velocities of muscles and ligaments. In the inverse DSEM measured subject rotations are translated to cadaver rotations. Anatomical data (inertia, parameters in the muscle model) for the DSEM are based on measurements on the cadaver of an 57-year old embalmed male [2]. A full description of the model is given elsewhere [20, 21, 25]. The DSEM can be used in different ways to predict muscle forces. It can be done by using either a *forward* or *inverse* dynamical modelling approach and will be referred to as the inverse or forward *mode* of the DSEM.

1.2. Forward dynamics

Although the relationship between muscle input (neural activation or excitation) and output variables (eg. force or energy expenditure) is complex and not completely understood, a muscle model (fig. 1) tries to mathematically describe this relationship. Among other factors, this relationship is dependent on force-length-velocity characteristics of the muscle. Neural input can not always be measured and parameters in the muscle model are difficult to measure *in vivo*. To validate force prediction from a muscle model, joint moments and resulting movements of and external forces on the skeleton can be calculated and compared to measurements of external forces and movements (kinematics). This however requires an anatomical description of the joints (moment arms of muscles with respect to joints they cross), an estimation of parameters in the muscle model and a mechanical description of the skeleton (skeleton dynamics).

Values for (joint-angle dependent) muscle moment arms in the DSEM are based on measurements of origin and insertion sites of all 31 muscles crossing shoulder and elbow joints on a human cadaver [25]. Muscles with large attachment sites are subdivided, resulting in a number of 139 muscle elements [23]. For each element some muscle parameters (mass, physiological cross-sectional area, optimum fibre length, tendon length) were measured as well. The *skeletal model* in the DSEM relates net joint moments to movements and external forces of the skeleton and is a finite-element model where each element is represented by an appropriate structure. In the calculation segment masses and inertia are used, which are based on cadaver data [25].

Usually neural activation can not be measured for all muscles in the musculoskeletal model, so these have to be assumed. Neural activation is parametrised and from an initial estimation of the input parameters (describing the shape of a muscle's neural activation) the resulting motion and external forces are calculated and compared with a motion and force recording. If a difference exists, in the next step of the optimisation muscle activations are altered until predicted and measured motion coincide sufficiently. Not only activation patterns can be optimised with *forward dynamical optimisation*; by allowing muscle parameters in the muscle model to vary, optimal values for these parameters can be found as well. For submaximal tasks more than one set of parameters might satisfy the optimisation criterium. To select one set, assumptions have to be made, but these assumptions can be hard to validate.

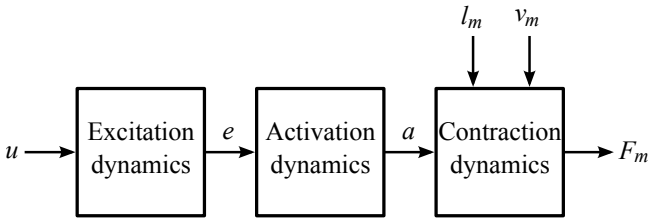

Figure 1: A forward muscle model is a mathematical description of the relationship between muscle force (F_m), excitation (e), activation (a), hypothetical neural input (u) and muscle force and velocity (l_m, v_m).

'Optimal values' in this case refer to values that result in the best fit of the model on recorded kinematics or net joint moments. When only a limited number of parameters is optimised and reasonable assumptions on neural activation can be given for each muscle in the system, forward dynamical optimisation can be a useful method for analysing muscle function. However, in large-scale musculoskeletal models involving multiple joints and many muscles, the number of parameters in the optimisation can become very large. Care should be taken in defining what muscle and input parameters are optimised. If many parameters compared to the number of measured datapoints are allowed to vary, the physiological interpretation of these can be doubted. Not only for this reason is decreasing the number of parameters important; computation times also set limits. Computational effort increases significantly with number of parameters in the optimisation. It is therefore often necessary to reduce the solution space by limiting the number of variables in the optimisation.

For predicting muscle forces with large-scale musculoskeletal models, another method is therefore often preferred.

1.3. Inverse Dynamic Optimisation

Inverse dynamics (see fig. 2) approaches the problem from the other end: kinematics and external forces are input and net joint moments are calculated using (inverse) skeleton dynamics. The next step to determine how muscles share the load has to deal with the problem of *redundancy* in the joints. More muscles than degrees of freedom (DOF) are present, implying that different sets of muscle forces will generate the same net joint moments. Additional information is required to determine what set of muscle forces from the solution space is selected. To select

one set, assumptions are made on the strategy the human brain uses to recruit muscles. Different criteria are used, but all look for a solution where a certain variable is minimised, eg. muscle stress [22] or energy expenditure [18].

Selecting a set of muscle forces by minimising a certain cost function is called *inverse dynamic optimisation* or *IDO*. The optimisation produces a solution that satisfies all constraints and recruits the 'cheapest' muscles for performing the movement. Inverse optimisation is computationally much more efficient than forward dynamics and has become the standard in large-scale musculoskeletal modelling. Validation of inverse dynamical models is mainly based on electromyographic (EMG) recordings of muscles. When the model predicts force and the simultaneously measured EMG shows muscle activity, the model is assumed to have found an adequate solution. Validation is only based on comparison of measured and predicted on-off-patterns, but magnitude of muscle force prediction can not be evaluated.

Whether the underlying assumption on recruitment strategy is true or the same for every human can hardly be verified. Even in healthy subjects significant inter-individual differences in recruitment strategies are observed but can not be accounted for by the IDO-mode of the DSEM. These differences can partly be subscribed to inter-individual morphological differences. [18]

Cocontraction — simultaneous agonist and antagonist action — is frequently observed and is thought as a form of active joint stabilisation by the muscles. Another limitation of inverse optimisation is that it is a bad predictor of cocontraction. If for example an elbow flexor produces a moment of 15 Nm about the elbow joint but an elbow extensor generates an opposing moment of 10 Nm, the net joint moment is 5 Nm. This is the moment that will be calculated from the inverse skeleton dynamics. The optimal solution in terms of minimal energy expenditure or lowest maximal muscle force or stress would be a muscle force in the elbow flexor that produces a moment of 5 Nm and no force generation in the elbow extensor. This is a very simplified example; a 1-DOF joint with only two muscles acting on that joint while most muscles act on multiple DOFs and most joints are 2- or 3-dimensional. In more complex models, problems might be less harsh because cocontraction might just occur because muscles act around multiple DOFs and always produce moments in other than desired directions, which have to be compensated for by other muscles.

The optimisation procedure is purely mathematical. In an unconstrained optimisation very high forces can be predicted for muscle elements that have favourable moment arm with respect to a joint. However, a muscle can not produce infinite force, can only produce force at a range of lengths (roughly between 60% and 140% of its optimum length) and can only work in one direction. In the inverse optimisation these muscle properties can be represented by upper and lower bounds on predicted muscle forces as linear inequality constraints. In the IDO mode

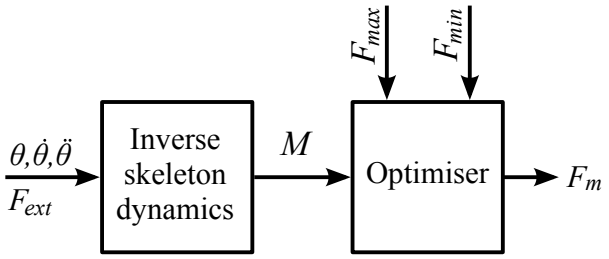

Figure 2: In the Inverse Dynamic Optimisation mode kinematics and external forces are input to skeleton dynamics, where joint moments are calculated. An optimisation procedure where a cost function is minimised leads to muscle forces. The solution space can be decreased by adding minimum and maximum boundaries on optimised muscle forces, which mathematically are described as linear inequality constraints.

of the DSEM lower bounds on all muscle forces are zero, the upper bounds are the product of a muscle's physiological cross-sectional area (PCSA), maximum muscle stress σ_{max} (constant for all muscles, in DSEM a value of 100 N/cm^2 is adopted) and maximum relative force ($F_{rel,max}$ the maximum force it can produce at its current length).

Adding constraints based on physiological properties decreases the solution space of the optimisation and can be expected to result in predictions that coincide better with reality.

1.4. Inverse Forward Dynamic Optimisation

Although the muscle force boundaries in the IDO mode force the optimisation to find a physiologically more feasible solution, two other muscle properties that might play an important role in dynamic movements are not taken into account:

- An electromechanical delay between muscle stimulation and force production exists, implying that the force of a muscle can not instantly rise from zero to its maximum value (or drop vice versa). This delay is caused by the neural command from the brain that needs some time to arrive at the muscle's membrane and the flow of calcium through the fibre's membrane, which is necessary for the muscle to form cross-bridges (and to produce force).
- Maximum muscle force is not only length- but also velocity-dependent [11].

Not including these dynamical properties of muscles in the optimisation might lead to erroneous predictions, especially for fast movements when the force-length-velocity characteristics of a muscle are expected to play a major role and muscle forces might rise and drop fast. In the forward dynamical mode (see 1.2) muscle dynamics are represented in a muscle model (fig. 1) that accounts for electromechanical delay and force-velocity-behaviour of the muscle. To include muscle dynamics in the computationally efficient inverse optimisation procedure, for this

study a combination of methods has been developed that further constrains the inverse optimisation by setting more strict limits on optimised muscle forces based on the forward muscle model described in Appendix A. This mode is called *Inverse Forward Dynamical Optimisation* or in short *IFDO*.

1.5. EMG-assisted modelling

The modes discussed so far use kinematics and external forces as input (IDO and IFDO) or to find optimal values for parameters in an optimisation procedure (forward mode). EMG-recordings are used for validation of the load sharing criterium. Often differences in on-off patterns are observed between EMG and predicted forces, indicating that the human brain recruits other muscles for performing a movement than the IDO mode predicts.

To account for individual differences, Buchanan & Lloyd [3, 4] developed a forward dynamical model for predicting knee joint moments in exercise and sports that uses both EMG and kinematics as input. First, muscle forces are calculated in a muscle model with processed EMG for all muscles together with muscle length and velocity as input. From these forces net joint moments are calculated (EMG predicted moments). Joint moments are also estimated from an inverse dynamical approach with recorded kinematics and external forces as input (inverse predicted moments). In some calibration trials parameters that describe the EMG-force relationship are tuned to obtain the best fit of the EMG predicted on inverse predicted joint moments. The calibrated EMG-force-model is then used with EMG as input to predict individual muscle forces for other than the calibration tasks.

This model does not make use of minimisation of a certain cost function to solve the load sharing problem and therefore does not rely on underlying assumptions on recruitment strategy. In contrast to inverse optimisation where each individual is assumed to use the same recruitment strategy, this method is able to model specific activation patterns. The method was applied at the knee for running and cutting maneuvers [15]. Individual muscle forces and EMG predicted net joint moments were calculated and compared to inverse predicted joint moments. Small differences of around $12Nm$ (when peak moments of $200Nm$ were found), concluding that this *EMG-driven* method is promising for predicting tissue loading in sports and exercise.

When this method is applied to the DSEM for dynamic tasks some problems occur. Many muscles crossing shoulder and elbow lie too deep under the skin to measure EMG from with surface electrodes. Intramuscular wire-electrodes can not be applied for dynamic tasks with a large range of motion. To some extent, Buchanan & Lloyd dealt with the same problem for the knee, where EMG from 3 out of the 13 muscles crossing the knee joint could not be measured. For these 3 muscles EMG was assumed to be equal to that of a synergistic muscle. In the shoulder a clear distinction between agonists and antagonists is not observed [24], which makes it impossible to make similar assumptions.

To use EMG as input to the the DSEM another method is therefore used. Muscle excitation can be interpreted as the neural signal arriving at the membrane and can be thought of as the same physiological quantity that is represented by rectified, filtered EMG (normalised to maximum EMG values). By assuming the excitation-force-relationship is equivalent to the EMG-force-relationship, forces for muscles where EMG was measured from can be calculated with a forward muscle model. These forces can then be used to constrain the inverse optimisation (see 2.1.4 and fig 3). In contrast to the model developed by Buchanan & Lloyd, EMG is not used to *drive* the model, but to assist the inverse optimisation in finding a solution that matches individual strategies. Therefore, this method is called *EMG-assisted*.

2. Methods

2.1. Model modification development

The modifications that led to the new modes are described here. All modes make use of a cost function to solve the load sharing problem, but they differ in the way boundaries on an inverse optimisation procedure are set as is depicted in Table 1. Upper and lower boundaries are represented by linear inequality constraints on the inverse optimisation. For DSEM users, a short tutorial on how to use the modes can be found in Appendix C.

2.1.1. IDO-mode

The inverse mode of the DSEM was adapted so not only muscle force is predicted, but muscle excitation and activation as well. By using an inverse muscle model with optimised muscle force at timestep i ($F_{m,i}$) and a muscle's state at timestep $i-1$ as input, activation a_i and excitation e_i are calculated. Calculating excitation from the optimised muscle forces allows direct comparison between measured EMG and predicted excitation and therefore provides a more quantitative validation criterium then muscle force on/off-patterns.

2.1.2. IFDO-mode

The IFDO mode differs from the IDO mode in the way the boundaries on optimal muscle forces are defined (see fig 3). From measurements of external forces and kinematics (input), joint moments are calculated with inverse dynamics. To constrain the load sharing problem, boundaries on muscle forces are calculated in a forward muscle model.

In the IFDO-mode, minimum and maximum bounds in timestep i of the optimisation are dependent on the muscle state (activation and length of contracile element), force in the previous timestep $i-1$ and excitation at timestep $i-2$, thereby preventing the predicted forces to rise or drop

Table 1: Minimum and maximum muscle forces can be represented by linear inequality constraints on the optimisation. In the EMG-modes bounds on muscle elements where EMG is measured from are calculated by setting EMG equal to excitation (column 'EMG'). For muscles where EMG is not measured from (column 'no EMG'), the constraints are defined by dynamic muscle force boundaries as in IFDO (EMG1) or as in IDO (EMG2).

	F_{min}		F_{max}	
Mode	EMG	no EMG	EMG	no EMG
IDO	0		$F_{rel,max} \cdot PCSA \cdot \sigma_{max}$	
IFDO	Muscle model with $u = 0$		Muscle model with $u = 1$	
EMG1	Muscle model with $e_{min} = EMG$	Muscle model with $u = 0$	Muscle model with $e_{max} = EMG$	Muscle model with $u = 1$
EMG2	Muscle model with $e_{min} = EMG$	0	Muscle model with $e_{max} = EMG$	$F_{rel,max} \cdot PCSA \cdot \sigma_{max}$

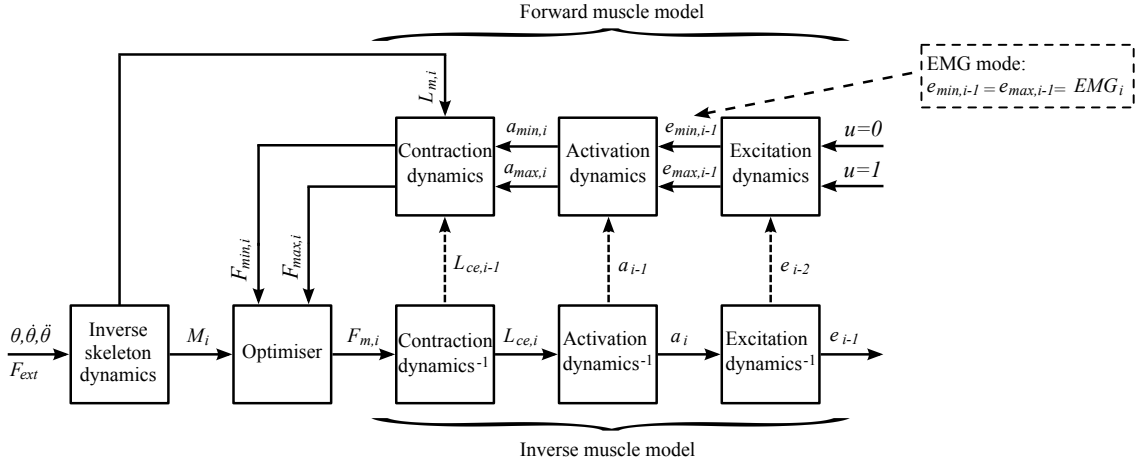

Figure 3: The IFDO is different from the IDO mode in that it uses a forward muscle model to set bounds on optimised muscle forces. Starting from the top right of the figure, neural input $u = 0$ and $u = 1$, together with a muscle's state in the previous timestep $i - 1$ are input to a forward muscle model to calculate minimum respectively maximum muscle force $F_{min,i}$ and $F_{max,i}$ for the current timestep. After optimisation, predicted muscle forces $F_{m,i}$ are input to the inverse part where length of the contractile element $L_{ce,i}$, activation a_i and excitation e_{i-1} are calculated, which can be used to set boundaries on the next time step. In the EMG mode both minimum and maximum excitation in the forward part for muscles where EMG is available from is set equal to measured EMG, resulting in the same minimum and maximum force ($F_{min,i} = F_{max,i}$). Hence, this muscle force is constrained to a fixed value and eliminated from the optimisation.

more rapidly than physiologically possible. By including the muscle model to set limits on the inverse optimisation, electromechanical delay between muscle activation and force production, as well as force-velocity-characteristics are taken into account.

2.1.3. Muscle model

Most muscle models that are used in large-scale musculoskeletal modelling are based on the phenomenological models proposed by A.V. Hill [11]. Models of different complexity are in use, but state-of-the-art models used for predicting muscle forces in dynamic movements incorporate at least a muscle's force-length-velocity characteristics. The muscle model in the DSEM (fig. 1) is a Hill-type model based on the work of Winters & Stark [27] and adapted by Happee [9]. A full description is presented in Appendix A, but a short overview of the main components is given here.

1. *Excitation dynamics* describe the relation between a hypothetical neural input u and the excitation of the muscle e, i.e. the neural signal which arrives at the muscle membrane. The latter is assumed to be comparable with normalised and filtered EMG. Mathematically it is described by a linear first-order system with time-constant τ_{ne}.

$$\frac{e}{u} = \frac{1}{1 + \tau_{ne} \cdot s} \tag{1}$$

2. *Activation dynamics* can be interpreted as the calcium flow through the muscle membrane. Again a linear first-order system is used to describe the relation between excitation e and muscle activation a. Calcium inflow is faster than calcium outflow and therefore two different time-constants are used for activation (τ_{ac}) and deactivation (τ_{da}):

$$\frac{a}{e} = \frac{1}{1 + \tau_{ac} \cdot s} \tag{2}$$

$$\frac{a}{e} = \frac{1}{1 + \tau_{da} \cdot s} \tag{3}$$

3. *Contraction dynamics* form the actual muscle part of the model. The muscle is modelled as a contractile element (CE) in series with a non-linear passive series-elastic element (SE). This chain is in parallel with a non-linear passive parallel-elastic element (PE). The CE is an active element, in which force development is a function of the non-linear force-length-velocity relationship.

First, for each muscle element the minimum boundary on excitation $e_{min,i-1}$ is calculated in eq. 1) with input e_{i-2} and hypothetical neural input $u = 0$. Eq. 2) will give current minimum activation $a_{min,i}$ by using the activation in the previous timestep a_{i-1} and $e_{min,i-1}$ as input. Minimum force $F_{min,i}$ is then obtained from the part of the muscle model that describes contraction dynamics with $l_{ce,i-1}$, the length of the contractile element at $i-1$ and current muscle length $l_{m,i}$ as input. Maximum force $F_{max,i}$ is calculated in a similar fashion, but by assuming the maximal hypothetical neural input of $u = 1$. Output of the optimisation procedure — optimised muscle forces — together with the muscle's state in the previous timestep ($l_{ce,i-1}$ and a_{i-1}) is then input to an inverse muscle model, where the current state is updated and excitation e_{i-1} is calculated so these can be used for setting boundaries on the next timestep.

2.1.4. EMG-modes

Instead of calculating bounds on a muscle's excitation, in the EMG-modes both minimum and maximum excitation of (some) muscle elements are set equal to measured EMG (see fig. 3). For each muscle element where EMG is measured from, a single value is calculated in a forward muscle model that is both used as minimum and maximum limit for that muscle element ($F_{min} = F_{max}$). By doing so, the muscle force for these elements are constrained to one single value, so no variation is allowed.

The EMG-mode allow the use of EMG for only some muscles, so it is not necessary to measure EMG for all muscles in the model. The EMG-mode has been developed in such a way that it can be defined to what muscle elements a measured EMG-signal corresponds to. For some smaller muscles with only a few elements in the DSEM it can be assumed that EMG that was measured on one location on that muscle is comparable to activity of all elements in that muscle. But for larger muscles (eg. M. Deltoideus or M. Serratus Anterior) this assumption is not reasonable and EMG should only be assigned to those element that anatomically correspond best to the location on the body where the electrodes were placed on[1].

Two modes that make use of these EMG-based constraints have been developed and are named the EMG1 and EMG2 mode. EMG1 and EMG2 differ in how bounds for muscle elements where EMG is not measured (or not switched on) from are defined. EMG1 uses boundaries as in IDO ($0 < F_m < F_{rel,max} \cdot PCSA \cdot \sigma_{max}$), while in EMG2 these elements are constrained by the dynamic bounds as in IFDO (so by using a forward muscle model with hypothetical neural input $u = 0$ and $u = 1$).

2.2. Data collection

Two datasets were used for this study. One was specifically measured for this study (subject 1) and will described in the next sections. The other dataset was measured on a patient (subject 2) with a shoulder endoprosthesis who was tested for another study (see [7] for test protocol). From this dataset abduction and anteflexion data (kinematics and EMG) at two different speeds were used. Data processing for subject 2 was done in a similar fashion as for subject 1.

3D kinematics and EMG of 14 muscles (see 2) were collected from one subject (subject 1, male, age 26, athletic build) who signed for his informed consent. The test was performed at the Vrije Universiteit (VU) in Amsterdam. An Optotrak system (Northern Digital, Inc., Waterloo, Ontario, Canada) with 4 camerasensors was used to collect 3D kinematic data (sampled at 50 Hz) of 4 clusters of markers attached to thorax, humerus, forearm and scapula-locator (a three-bar linked system that is held on three scapular bony landmarks and is used to track scapular rotation [19]). Each cluster consisted of 3 markers. Clusters were attached to the skin with double-sided adhesive tape. The thorax cluster was placed on the sternum, the humerus cluster on the lateral arm just below the insertion of the deltoid and the forearm cluster just proximally to the ulnar and radial styloid. The subject's acromion shape did not allow the use of a marker cluster to track scapular motion, because no flat surface was present to attach the marker cluster to without introducing large inaccuracies due to skin movement. Instead a scapula-locator was used to track scapular motion during the experimental tasks at slow, medium and fast speed (see 2.3). For the tasks at maximum speed this was not possible, because movements were too fast to position the scapula-locator correctly.

Surface electrodes were placed on 14 muscles (interelectrode distance of 20 mm) and connected to a 16-channel Porti System (TMS International, Enschede, The Netherlands). EMG data were sampled at 1000 Hz and analogue band-pass filtered (cut-off frequency 5-400 Hz).

2.3. Experimental tasks

2.3.1. Static tasks

Measurements were done to determine static scapular and clavicular rotation during anteflexion and abduction (static trials). The scapula-locator was held on three bony landmarks of the scapula (trigonum spinae (TS), angulus inferior (AI) and angulus acromialis (AA)) while the subject elevated his arm at intervals of approximately 15°. At

[1] Also, it is not necessary to use EMG for all the muscles that have been measured. By simple changes in the input-files EMG channels can be switched on or off. See Appendix C

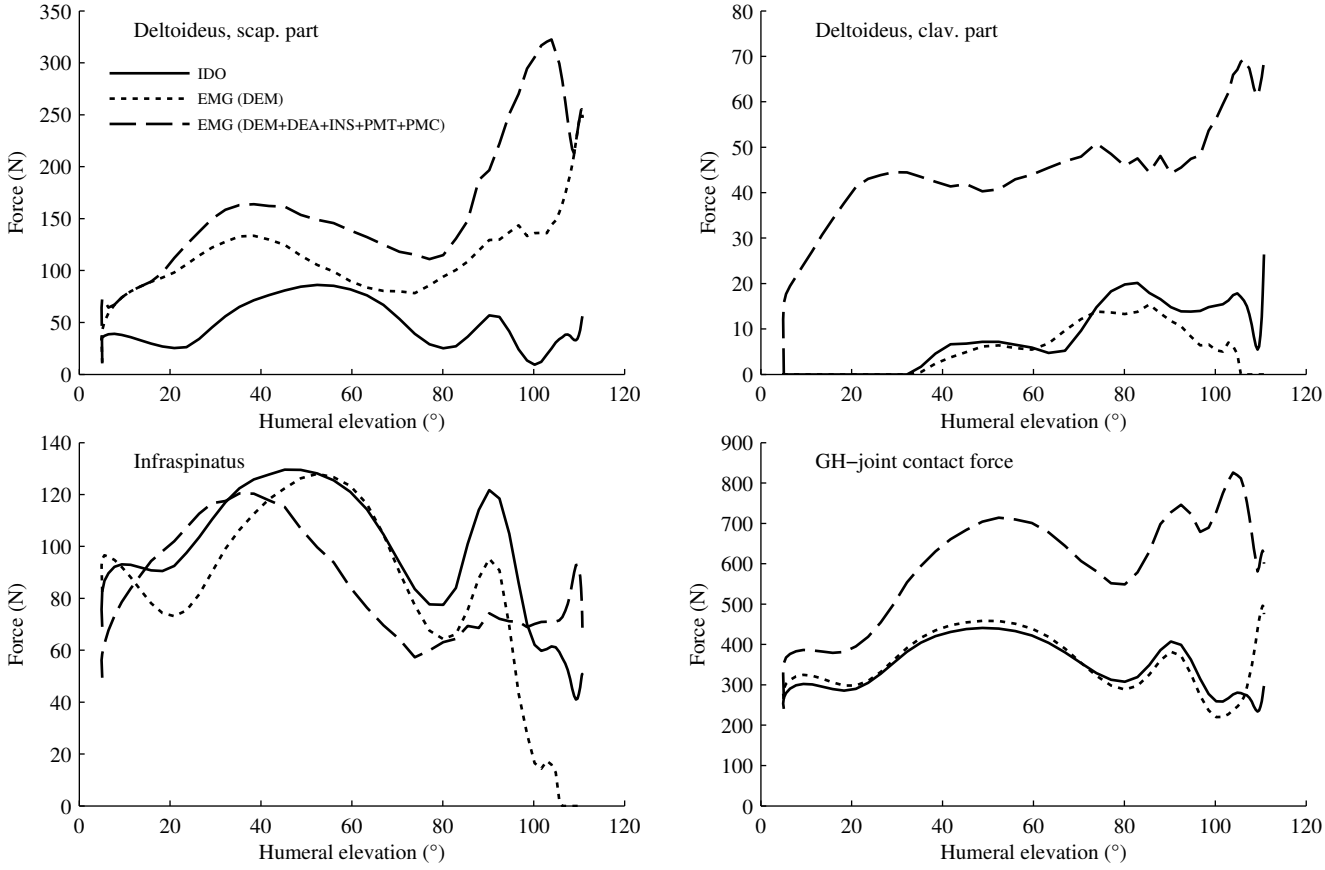

Figure 4: Force prediction for M. Deltoideus (scapular and clavicular part), M. Infraspinatus and GH-joint contact force for an anteflexion movement in IDO and EMG mode. Adding only EMG for DEM results in higher forces for DEM, but decreases force prediction for DEA. When also EMG is added for DEA, INS, PMT and PMC force predictions are further increased. This is also reflected in higher GH-joint contact force, especially for higher elevation angles.

each position the arm was held still for approximately 2 seconds. This calibration procedure was performed twice for abduction and twice for anteflexion.

2.3.2. Dynamic tasks

By mimicking the person in front of him, the subject performed two different motions: shoulder anteflexion (FL) and shoulder abduction (AB) from resting position (arm hanging vertical down) to approximately 120° humeral elevation and back. Both movements were performed at four different speeds: slow (SL), medium (MED), fast (FA) and maximum speed (MAX). The slow motions were timed on a stopwatch to take 4 seconds to get from resting position to maximal humeral elevation and 4 seconds to get back again to the resting position. For medium and fast motions this time was respectively 2 and 1 second. For the motions at maximum speed the subject was instructed to elevate his arm as fast as possible. Each combination of movement and speed was performed three times, resulting in a total of 24 recordings.

2.3.3. MVC tasks

To induce maximum activity for muscles where EMG was measured from, 10 isometric maximum voluntary contractions (MVC) tasks were performed. Each task was done twice for approximately 3 seconds with at least 60 seconds rest in between trials. The 4 tasks suggested by Boettcher [1] were performed as well as the following 6 tasks: elbow flexion with elbow 110° flexed, elbow extension with elbow flexed at 10° and 90°, shoulder anteflexion, retroflexion and abduction with the elbow stretched and the arm hanging vertical down. Counteracting forces were applied at the subject's wrist by a strap which was connected to a rope and was handheld by an assistant on the other end.

2.4. Data processing

3D marker data were transformed to segment coordinate systems according to DSEM convention, which is equal to ISB convention [28], except that all coordinate systems are rotated 90° around the y-axis so that in the anatomical position the x-axis points to the right, the z-axis posteriorly and the y-axis superiorly. Input to the DSEM is formed

Table 2: Muscles of which EMG was measured and their abbrevations. To allow comparison between EMG and DSEM-predictions, EMG-channels are assigned to one or a few muscle elements that anatomically correspond best to the position on the skin where electrodes were placed. The last two columns present the first (F) and last (L) elements to which the EMG channel was assigned. Element numbering can be looked up in table C.4. In the DSEM the M. Deltoideus is subdivided in two parts: the scapular and clavicular part. The clavicular part represents the more anteriorly located muscle fibres that have insertion sites on the clavicula, and is therefore referred to as M. Deltoideus, anterior part (DEA). Because on the scapular part two electrode pairs were placed, this muscle is subdivided in a posterior part (DEP, elements 80-85) and a medial part (DEM, elements 86-90).

#	Muscle	Abb.	F	L
1	M. Pectoralis major clav. part	PMC	145	146
2	M. Pectoralis major thor. part	PMT	139	144
3	M. Deltoideus post. part	DEP	80	85
4	M. Deltoideus ant. part	DEA	91	94
5	M. Deltoideus med. part	DEM	86	90
6	M. Trapezius scap. part	TRS	48	51
7	M. Trapezius clav. part	TRC	55	56
8	M. Biceps brachii, long head	BIB	126	126
9	M. Triceps brachii, lat. head	TRL	173	177
10	M. Infraspinatus	INS	98	103
11	M. Serratus anterior	SEA	68	72
12	M. Latissimus dorsi	LAD	134	137
13	M. Brachioradialis	BRA	160	162
14	M. Teres major	TEM	107	110

by time series of cardan angles of the rotation of the thorax relative to the global coordinate system (order: X-Y-Z), clavicle to thorax (Y-Z-X), scapula to thorax (Y-Z-X), humerus to thorax (Y-Z-Y), forearm to humerus (X-Z-Y) and 3D position of the incisura jugularis (IJ).

EMG were band-pass filtered (zero-phase forward and reverse pass 2nd order Butterworth filter, band-pass frequency 10-400 Hz), rectified, low-pass filtered (zero-phase forward and reverse pass 2nd order Butterworth filter, cut-off frequency 3 Hz), normalised to maximum values obtained in the MVC trials and resampled to the frequency at which kinematics were measured (50 Hz).

With humeral elevation as independent variable, 5th-order polynoms were fitted on the 6 scapular and clavicular angular rotations (relative to thorax) based on the static trials (2.3.1). Two polynoms were fitted: one for anteflexion and one for abduction. For the dynamic trials (2.3.2) with the scapula-locator measured angular rotations were compared to the polynom-fitted angular rotations. Between polynom-fitted angles and measured angles as well as in between measured angles during different dynamic trials (of same speed and movement) large deviations were found ($> 15°$). It was concluded that the scapula-locator was not held at the right position during the dynamic trials and that measured angles during the dynamic trials could not be trusted. Therefore, for all movements polynom-fitted angles were used.

From all recordings only the lifting phase (from resting position to maximal humeral elevation) was analysed.

2.5. Model simulations

First, from all 24 recordings (2 movements, 4 speeds, each combination 3 times) limb accelerations and net joint moments were calculated. To predict muscle forces and joint reaction forces an inverse optimisation procedure was followed with different boundaries on muscle forces according to the described modes (IDO, IFDO, EMG). As optimisation criterium a cost function was used that looks for minimum energy expenditure in the muscle[18]:

$$J = \sum_{i=1}^{n} F_{m,i} l_{m,i} + m_i c_1 \left(\frac{F_{m,i}}{F_{rel,max}(l)} + c_2 \left(\frac{F_{m,i}}{F_{rel,max}(l)} \right)^2 \right) \tag{4}$$

in which $F_{m,i}$ is muscle force, $l_{m,i}$ muscle length, m_i muscle mass and $F_{rel,max}$ the maximum muscle force the muscle i can produce at its current length. The total cost is the sum over all muscle elements n. Constants c_1 and c_2 were chosen to be 100 and 4.

2.6. Evaluation criteria

Difference between measured EMG and predicted excitation e is represented by the root mean square error:

$$RMSE = \sqrt{\frac{\sum_{j=1}^{n_s} (e_j - EMG_j)^2}{n_s}}, \tag{5}$$

where n_s is the number of samples in the signal.

For larger muscles with multiple muscle elements, excitation was averaged over the element that anatomically corresponded best to electrode placement and some (maximum 5) of its neighbouring elements. In table 2 it can be looked up to what muscle elements the EMG channels were assigned.

An RMSE of 0 would mean perfect correspondence between measured EMG and predicted excitation. Deviations from zero can be explained by three factors: 1) false positive: excitation is predicted while no EMG is measured, 2) false negative: no excitation is predicted while EMG is measured, 3) difference in magnitude between EMG and excitation.

3. Results

The DSEM crashed on the measured data (error 0: Check input kinematics) for subject 1, because in the kinematical part measured rotations could not be translated to cadaver rotations. Morphological differences between cadaver (number 'l1091') and subject 1 were large and most pronounced in difference in thorax size in anterior-posterior direction ('thorax depth'). Before simulations could be run, thorax depth was scaled by a factor of 0.88

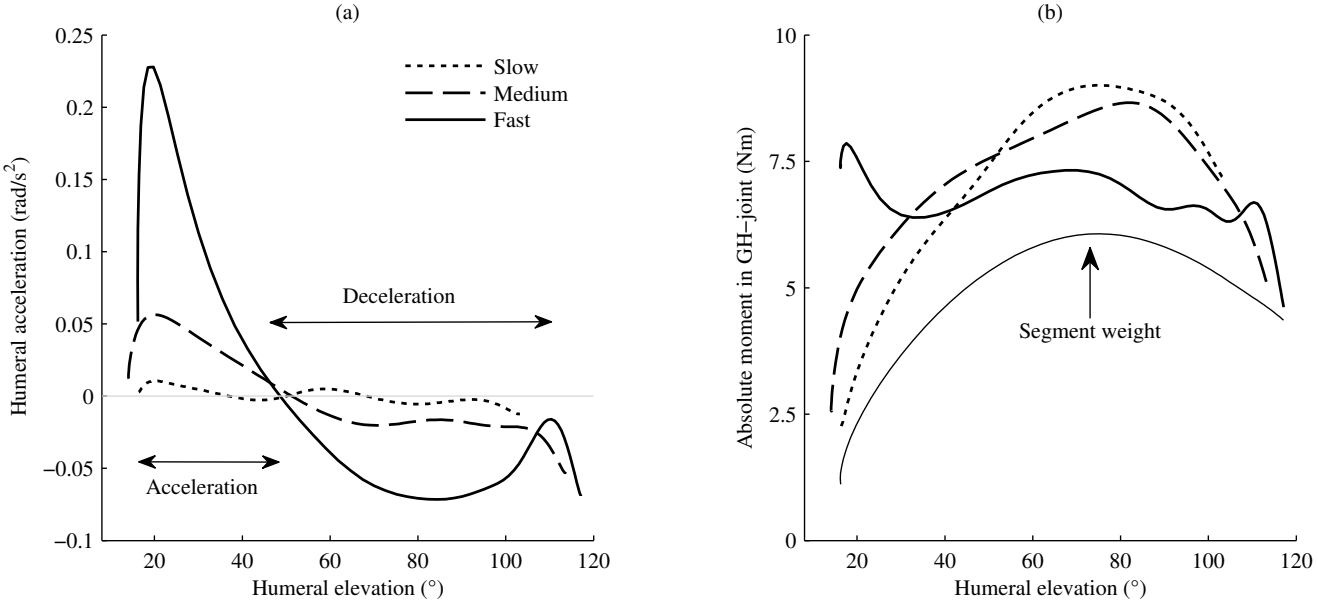

Figure 5: During abduction and anteflexion, net joint moments are produced around the GH-joint to overcome gravity and to accelerate the arm. At slow and medium speed gravity contributes most to maximum joint moments. At fast and maximum (not shown) speed accelerative terms play a major role and maximum joint moments are found in the acceleration phase at low elevation angles.

and conoid length was shortened from 1.94cm to 1.18cm before simulations could be run. See Appendix B for a full description of these changes.

Table 3 and fig. 5 show some characteristics of the different speeds of movement execution. The highest moments in the GH-joint were predicted in the acceleration and deceleration phase for movements at maximum speed.

In the IDO-mode RMSE was largest for muscle DEA and INS. For both movements, predictions became worse when speed of movement execution increased. At slow speed, the RMSE averaged over all muscles was 0.058, while at medium, fast and maximum speed this increased to respectively 0.066, 0.078 and 0.213. Force predictions showed similar patterns for slow, medium and fast speed movements. RMSE for anteflexion were a little lower than for abduction. During abduction false negatives were predicted for INS for almost the complete movement. For almost all muscles, excitation was predicted to be higher than measured EMG.

For all recordings at maximum speed (except for one anteflexion recording), the DSEM could not find a solution for some samples in the recordings[2]. The predicted joint moments could not be produced by the muscles. The samples where no solution could be found for were generally found in the acceleration phase and/or deceleration phase when joint moments were maximal.

In the IFDO-mode for both movements and at all speeds no solution could be found for some samples in the recordings. To verify that the method theoretically works, data for an anteflexion and abduction movement at two different speeds from subject 2 were used to validate the working principle. From the 28 recordings only 5 could be run without errors. For the other recordings no solution could be found in the optimisation. Fig. 7 shows the boundaries and predicted muscle force for one element based on IDO and IFDO for an abduction movement that could be run without errors. Muscle force boundaries in IFDO were much stricter than in IDO. For the recordings where the DSEM gave positive results for, difference between minimum and maximum force in IFDO was decreased by on average 83% compared to IDO.

Because the model could not find a solution in the IFDO mode for all data from subject 1, running simulations in the EMG1 mode that only constrains the optimisation more was not successful either. In the EMG2 mode often no solution could be found for the linear constraints when EMG was added. Different combinations of muscles have been tried, especially muscles that showed large difference between predicted excitation and measured EMG (DEA, INS), but no significantly different results from IDO were found.

To validate the effect of adding EMG, again data from subject 2 were used. Fig. 4 shows muscle force prediction in the IDO mode and EMG mode (EMG2 mode, with two different combinations of EMG) for some muscles and the GH-joint contact force (which is dependent on all muscles crossing the GH-joint). Adding EMG for DEM (part of Deltoideus, scap. part) leads to higher force prediction, mainly at higher humeral elevation (>90 °). This is also reflected in higher GH-joint contact force. When also EMG for DEA, INS, PMT and PMC are added, forces in

[2]Error MINNL: item 1 - No solution can be found for the linear constraints.

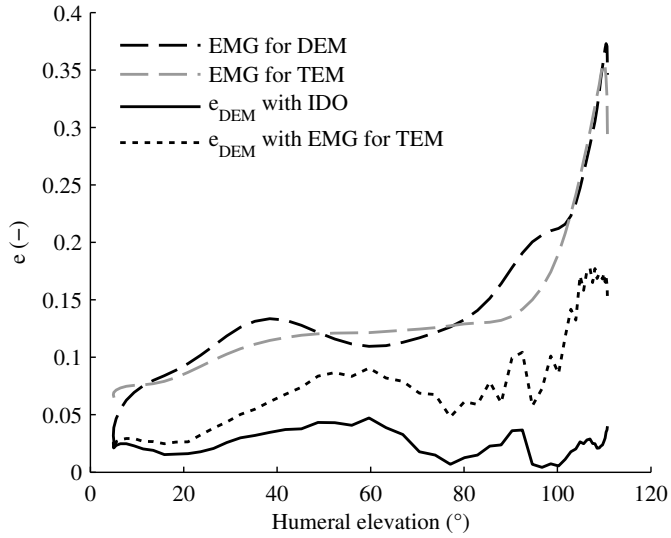

Figure 6: For an anteflexion measured on subject 2, the IDO mode predicted no force at all for TEM. However, EMG was measured. When this EMG was added to constrain muscle force prediction of TEM, better correspondence between measured EMG and predicted excitation was found for one of its antagonist muscles, namely DEM.

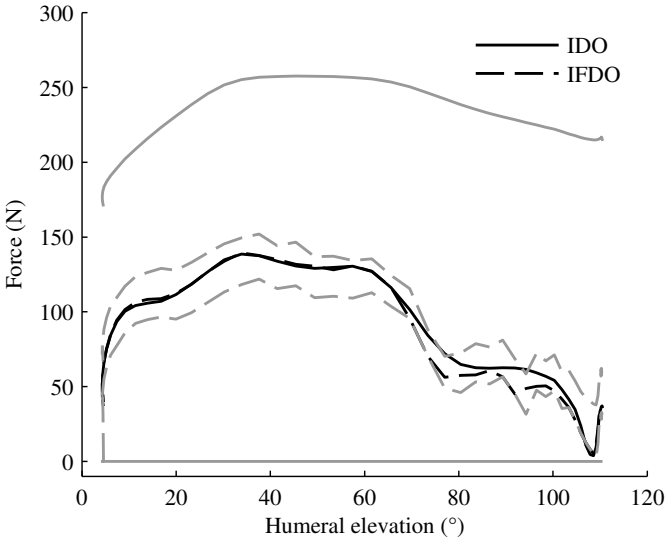

Figure 7: Muscle force prediction with the DSEM in IDO and IFDO for M. Supraspinatus (element 113) for an abduction movement. In the IFDO mode boundaries (grey) on muscle forces (black) are much stricter than in IDO. Force prediction between IFDO and IDO however did not differ much, but bounds on the optimisation were much stricter (on average 83%).

the GH-joint are predicted to be much higher over the full range, but still mainly at high humeral elevation angles. Instead of a peak force of $440N$ at 48° elevation, a value almost twice as high ($820N$) at 105° humeral elevation is predicted. RMSE decreased from 0.14 to 0.12 by adding DEM and further decreased to 0.0847 when the other muscles were added.

Another interesting result was found when EMG for muscle TEM was added to constrain the optimisation for an anteflexion movement measured on subject 2 (see fig. 6). EMG was added, because in the IDO mode no force was predicted for TEM while EMG was measured. Adding EMG for TEM also lead to improved prediction of DEM, an antagonist muscle. By adding EMG for TEM, RMSE for muscle DEM reduced from 0.1627 to 0.0417, and the pattern of predicted excitation coincides better with measured EMG than in the IDO mode. This also worked the other way around: adding EMG for DEM lead to improved prediction of TEM compared to IDO ($RMSE = 0.1986$ in IDO versus 0.1691 in EMG mode).

4. Discussion

Morphological differences play an important role in DSEM predictions. The kinematical part of the DSEM (the part that translates meaured rotations to cadaver rotations) only worked on subject 1 without errors after adapting some morphological parameters in the cadaver file (thorax depth and conoid length, see Appendix B). Especially shortening the conoid can not fully be explained by measurements and inspection of the results still showed some abnormal behavior. For example elements in muscle INS, a rotator-cuff muscle which has a moment arm in the desired direction around the GH-joint and is known to be activated during abduction in healthy persons, hardly produced any force according to DSEM. The reason for this was that INS was predicted to be out of its range where it could produce any force (<60% of its optimum length) for a significant part of the movement, and very short for the rest of the movement. Recruiting this muscle was therefore relatively expensive in the optimisation. Because EMG was measured for INS in all recordings, it can be concluded that the muscle produces some force and DSEM-predicted length is too short. By shortening the optimum fibre length for the elements in INS by 20% this problem was solved (muscle force was predicted during the complete movement), but this scaling factor can not be verified.

DEA is an important flexor of the arm, and although its length was within range and had moment arms in the desired direction around the GH-joint, almost no force was

Table 3: t = time to get from resting position (arm hanging vertically down) to maximum humeral elevation (appr. 120°). $\dot{\theta}_{max}$ = maximum angular velocity in the GH-joint, $\ddot{\theta}_{max}$ = maximum angular acceleration in the GH-joint, M_{max} = maximum absolute moment in the GH-joint, F^{GH}_{max} = maximum absolute GH-joint reaction force. Values are averaged over all 6 recordings (3x abduction, 3x anteflexion) per speed.

Speed	t (s) sec	$\dot{\theta}_{max}$ (rad/s)	$\ddot{\theta}_{max}$ (rad/s^2)	M_{max} (Nm)	F^{GH}_{max} (kN)
SL	±4.0	0.54	0.017	9.33	0.404
MED	±2.0	1.34	0.077	9.31	0.402
FA	±1.0	2.60	0.26	8.73	0.392
MAX	0.343	8.33	1.86	44.3	1.689

predicted for this muscle. Setting EMG for this muscle as a constraint on the optimisation would be an obvious choice. When this was done, force balance around the clavicula could not be found and the model could not find a solution for the optimisation problem. This is probably related to the changed conoid length: usually the conoid plays a significant role in the force and moment balance for the clavicula, but with the short conoid that was used for these simulations no conoid ligament forces were predicted. This explains the model crash when EMG for DEA was added.

At maximum speed the IDO mode crashed in all but one sample. Because the samples where the optimisation could not find a solution for were the samples where predicted joint moments were maximal, these joint moments were compared to moments at other velocities. To flex or abduct the arm, gravity must be overcome. At the start of the movement, flexors and abductors in the shoulder are activated to accelerate the arm until maximum velocity is reached. Subsequently the limb is decelerated by gravity and can be further decelerated by shoulder adductors and extensors until zero speed is reached at maximum humeral elevation of approximately 120°. In fig. 5a it can be seen that acceleration increases with speed of movement execution.

Net joint moments can be subdivided into two parts: a moment produced by the segment weight (gravity) and accelerative moments (inertial effects). As a result of higher limb accelerations, predicted joint moments in the acceleration phase (fig.5b) become higher when speed of movement execution increases. For movements at slow and medium speed segment weight is the dominating factor and peak moments are predicted when gravity on the arm produces maximum moment in the GH-joint (between 70° and 80° humeral elevation). As can be expected the accelerative moment plays a larger role at fast and maximum speed. In the moment-elevation curve at fast speed a second peak is observed when acceleration is maximal (at low humeral elevation). Both peaks in the curve are of equal order of magnitude. When the subject was instructed to abduct or flex his arm at maximal speed accelerations became much higher (1.88 rad/s^2, more than 7x higher than at fast speed) and this is also reflected in much higher maximum joint moments (44.3 Nm, 5x higher). Limb inertia is clearly the dominating factor in peak moment prediction at maximum speed. Both in the accelerative phase (at low humeral elevation) and in the decelerative phase (just before maximum elevation is reached) high moments are predicted.

The muscles crossing the GH-joint could not produce these moments. In other words: the subject could apparently lift his arm faster than the cadaver could have. The subject was of athletic build, so it is reasonable to assume that he indeed can lift his arm faster than the 57-year old man from which anatomical data for the DSEM were derived could have. To verify this assumption, simulations were done again, but now with a σ_{max} of $150N/cm^2$ (instead of $100N/cm^2$). This can be interpreted as a 1.5 times 'stronger' cadaver than the one measured. This did not only lead to less model crashes for the maximal trials, it also showed lower RMSE for the other speeds (on average 10%). This indicates that the subject was indeed stronger than the cadaver and also partly explains why excitation was overestimated (compared to measured EMG) for most muscles.

All of the above mentioned observations lead to the conclusion that morphological differences were the dominating factor in muscle force predictions for subject 1. The failure of the IFDO and EMG modes to find solutions to the optimisaton problem could most likely be subscribed to these differences. When differences between subject and cadaver are large, the model was found to face problems in translating subject to cadaver rotations. To make the DSEM more generic, it is advisable to further develop the anatomical dataset on which it is based. Taking into account morphological differences can also be achieved by developing more advanced scaling routines than the one available now (uniform scaling) and the one developed for this study (non-uniform scaling for the thorax).

Because dataset from subject 1 was not the best choice for validating the new modes, instead data from another subject was used. Data from subject 2 ran without problems in the IDO mode. In the IFDO mode only 5 out of 28 samples did not show errors. For these 5 trials, outcome was very comparable to IDO in most cases, although the solution space was significantly decreased (on average 83%). The reason for the many crashes can partly be related to the mathematical procedure that is followed to define the boundaries on the optimisation. If for some reason the model can not find a solution for one timestep it automatically sets all muscle forces to 0 for that timestep. Because maximum forces for the next step are based on these zero-forces and the maximum rise according to the muscle model, maximum bounds for the next step are very low. This means that if one sample fails, generally all samples will fail. This dependency is undesired, because also in IDO-predictions it is not uncommon to have one or a few 'bad' samples where no solution can be found for. In IFDO, the whole trial would fail.

Another downside of the IFDO mode is that it puts more emphasis on morphological parameters. Boundaries on all muscle forces are influenced by the parameters measured on one cadaver. If for some reason significant differences for one or a few muscles are present, this already might lead to no solution for the optimisation. Putting more and stricter physiologically based constraints on the optimisation would help in finding more realistic predictions. However, it also makes the model more sensitive to differences between subject and cadaver. Scaling to subject-specific values is therefore important before IFDO can be used. Scaling to eg. maximum strength (possibly in different directions) would be a good starting point. The data measured on subject 1 would have been a good dataset to tune some parameters on and to verify whether the IFDO

mode indeed accounts for velocity effects in muscle force prediction. Especially, it would have been interesting to see how IDO and IFDO predictions differ for movements at maximum velocity. Unfortunately, this dataset could not be used. The dataset for subject 2 did not include a large range of velocities and also in this set only 5 trials ran without errors.

More promising results were found when the inverse optimisation for subject 2 was constrained with EMG. Adding EMG for muscles where false negatives were predicted for led to higher predicted muscle forces. In all cases, excitation for the M. Deltoideus was underestimated (compared to measured EMG) for higher elevation angles. Adding EMG for this muscle (DEA for flexion, DEM for abduction, or add both) resulted in an increase in muscle force prediction at these higher elevation angles. This was also reflected in higher GH-joint contact force. Because other studies [7] suggest that GH-joint contact force is generally underestimated, adding EMG for the deltoids seems to lead to improved model performance.

For a few examples it has been found that EMG-based constraints indeed can account for cocontraction and individual patterns. A good example of this was given in fig. 6: adding EMG for DEM improved prediction for TEM, and vice versa. If more of these pairs can be found (and in more subjects), adding EMG from only one or a few muscles could lead to better predictions for both these and other muscles. Research should be focused on what combinations of EMG can be used best to account for observed cocontraction. The limited amount of data that has been used for simulations in this study suggests that adding EMG for the M. Deltoideus (for abduction and anteflexion) and Pectoralis Major (for anteflexion) is a good starting point. Measuring EMG in shoulder muscles is still hampered by the fact that many shoulder muscles lie deep under the skin (and thus can not be measured with surface electrode measurements). Not only is EMG relatively easy to measure from M. Deltoideus and Pectoralis Major, these are also often underestimated by the DSEM.

Another interesting topic for future research lies in developing calibration procedures for the EMG-force relationship. First of all, in this study it was assumed that processed EMG (normalised to maximum values) is equal to excitation. Although both variables theoretically represent the same signal (neural signal arriving at the muscle membrane), large deviations may occur because of several factors. Surface electrode measurements for some rotator-cuff muscles (INS, TEM, M. Supraspinatus) show large overestimations and offsets compared to measurements with intramuscular wire electrodes [26] (which measure inside the muscle belly and are therefore expected to give more accurate measurements). Quality of EMG for these muscles is therefore questionable. Also, the EMG-force relationship is known be dependent on muscle length and velocity. Whether the forward muscle model used in the DSEM accounts for this is hard to verify, because muscle forces can not be measured *in vivo*. Furthermore, it can not be verified whether true maximum values were obtained for all muscles during the MVC trials. However, mucsle force prediction is sensitive to these maximum values.

Summarising, two new modes for the DSEM have been developed that constrain the inverse optimisation with bounds based on forward dynamics and EMG. It has been proven that the IFDO mode works and narrows the solution space for muscle force prediction. However, the IFDO mode overconstrains the optimisation in many cases. Calibration and scaling routines should be developed before the IFDO mode can be used. The EMG-assisted mode can be used to account for individual differences and can predict cocontraction in other muscles than muscles for which EMG was used. Especially improvements to the EMG-assisted mode are an interesting topic for future research. However, morphological differences can play a dominant role in muscle force prediction with the DSEM. More anatomical data should be measured and scaling routines should be developed to make the DSEM more generic.

References

[1] C. E. Boettcher, K.A. Ginn, and I. Cathers. Standard maximum isometric voluntary contraction tests for normalizing shoulder muscle EMG. *Journal of orthopaedic research*, 26(12):1591–1597, 2008.

[2] M. D. Klein Breteler, C. W. Spoor, and F.C.T. Van der Helm. Measuring muscle and joint geometry parameters of a shoulder for modeling purposes. *Journal of Biomechanics*, 32:1191–1197, 1999.

[3] T.S. Buchanan, D.G. Lloyd, K. Manal, and T.F. Besier. Neuromusculoskeletal modeling: Estimation of muscle forces and joint moments and movements from measurements of neural command. *Journal of Applied Biomechanics*, 20:367–395, 2004.

[4] T.S. Buchanan, D.G. Lloyd, K. Manal, and T.F. Besier. Estimation of muscle forces and joint moments using a forward-inverse dynamics model. *Medicine & Science in Sports & Exercise*, 37(11):1911–1916, 2005.

[5] B.P. Cho and H.S. Kang. Articular facets of the coracoclavicular joint in koreans. *Acta Anatomica*, 163:56–62, 1998.

[6] C.J. DeLuca and W.J. Forrest. Force analysis of individual muscles acting simultaneously on the shoulder during isometric abduction. *Journal of Biomechanics*, 6:385–393, 1973.

[7] A.A. Nikooyan et al. Comparing model-predicted GH-joint contact forces by in-vivo measured forces. *Journal of Biomechanics*, 41 (Supplement 1):S145, 2008.

[8] Borivoye Gradoyevitch. Coracoclavicular joint. *Journal of Bone & Joint Surgery*, 21:918:920, 1939.

[9] R. Happee. *The control of shoulder muscles during goal directed movements*. PhD thesis, Delft University of Technology, 1992.

[10] R.I. Harris, H. Dzung, D.H. Sonnabend, and J.A. Goldberg. Anatomic variance of the coracoclavicular ligaments. *Journal of Shoulder and Elbow Surgery*, 10:585–588, 2001.

[11] A.V. Hill. The heat of shortening and the dynamic constants of muscle. *Proc. Roy. Soc. B*, 126:136–195, 1938.

[12] C. Hogfors, B. Peterson, G. Sigholm, and P. Herberts. Biomechanical model of the human shoulder - ii. the shoulder rhythm. *Journal of Biomechanics*, 24:699–709, 1991.

[13] C. Hogfors, G. Sigholm, and P. Herberts. Biomechanical model of the human shoulder - i. elements. *Journal of Biomechanics*, 20:157–166, 1987.

[14] H. Kaur and I. Jit. Coracoclavicular joint in northwest indians. *American Journal of Physical Anthropology*, 85:457–460, 2005.

[15] D.G. Lloyd and T.F. Besier. An EMG-driven musculoskeletal model to estimate muscle forces and knee joint moments in vivo. *Journal of Biomechanics*, 36:765–776, 2003.
[16] D.J. Magermans, E.K.J. Chadwick, H.E.J. Veeger, P.M Rozing, and F.C.T. van der Helm. Effectiveness of tendon transfers for massive rotator cuff tears: a simulation study. *Clinical Biomechanics*, 19:116–122, 2004.
[17] A model for the prediction of the forces at the glenohumeral joint. I. w. charlton and g. r. johnson. *Proceedings of the Institution of Mechanical Engineers, Part H: Journal of Engineering in Medicine*, 220:801–812, 2006.
[18] M. Praagman. *Muscle load sharing*. PhD thesis, VU Amsterdam, 2008.
[19] C. van Andel, K. van Hutten, M. Eversdijk, H.E.J. Veeger, and J. Harlaar. Recording scapular motion using an acromion marker cluster. *Gait Posture*, in press: , 2008.
[20] F.C.T. van der Helm. Analysis of the kinematic and dynamic behavior of the shoulder mechanism. *Journal of Biomechanics*, 27(5):527–550, 1994.
[21] F.C.T. van der Helm. A finite element musculoskeletal model of the shoulder mechanism. *Journal of Biomechanics*, 27(5):551–569, 1994.
[22] F.C.T. van der Helm and H.E.J. Veeger. Quasi-static analysis of muscle forces in the shoulder mechanism during wheelchair propulsion. *Journal of Biomechanics*, 29(1):39–52, 1996.
[23] F.C.T. van der Helm and R. Veenbaas. Modelling the mechanical effect of muscles with large attachment sites: application to the shoulder mechanism. *Journal of Biomechanics*, 24:1151–1163, 1991.
[24] H.E.J. Veeger and F.C.T. van der Helm. Shoulder function: The perfect compromise between mobility and stability. *Journal of Biomechanics*, 40:21192129, 2007.
[25] H.E.J. Veeger, F.C.T. van der Helm, L.H.V. van der Woude, G.M. Pronk, and R.H. Rozendal. Inertia and muscle contraction parameters for musculoskeletal modelling of the shoulder mechanism. *Journal of Biomechanics*, 24:615–629, 1991.
[26] D.L. Waite, R.L. Brookham, and C.R. Dickerson. On the suitability of using surface electrode placements to estimate muscle activity of the rotator cuff as recorded by intramuscular electrodes. *Journal of Electromyography and Kinesiology*, Article in press, 2009.
[27] J.M. Winters and L.S. Stark. Analysis of fundamental human movement patterns through the use of in-depth antagonistic muscle models. *IEEE Transactions on Biomedical Engineering*, 32:826–839, 1985.
[28] G. Wu, F.C.T. van der Helm, H.E.J. Veeger, M. Makhsous, P. van Roy, C. Anglin, J. Nagels, A.R. Karduna, K. McQuad, X. Wang, F.W. Werner, and B. Buchholz. ISB recommendation on definitions of joint coordinate systems of various joints for the reporting of human joint motion - Part II: shoulder, elbow, wrist and hand. *Journal of Biomechanics*, 38:981992, 2005.

Appendix A. Muscle model

This appendix describes the muscle model in the DSEM. It is based on the work of Winters & Stark [27] and adapted by Happee [9].

Excitation dynamics

Excitation dynamics describe the relation between a hypothetical neural input, thought of as a motor program of inifinte bandwith, i.e. it can be a pure step, and the excitation of the muscle, i.e. the neural signal which arrives at the muscle membrane. The latter can be compared with the EMG signal. It should be noted that the puls-type neural spikes are represented by a continuous signal.

$$\frac{e}{u} = \frac{1}{1 + \tau_{ne} \cdot s}, \tag{A.1}$$

where e is excitation, u is neural input and τ_{ne} time constant for neural excitation.

Activation dynamics

The activation dynamics describe the relation between muscle excitation e and muscle activation a and can be interpreted as the calcium flow through the muscle memebrane. Since calcium inflow is a much fater process than calcium outflow, the first-order system can be described with two time-constants:

$$\frac{a}{e} = \frac{1}{1 + \tau_{ac} \cdot s}, \tag{A.2}$$

$$\frac{a}{e} = \frac{1}{1 + \tau_{da} \cdot s}, \tag{A.3}$$

where a is activation, e is excitation, τ_{ac} time constant for activation ($e > a$) and τ_{da} time constant for deactivation ($e < a$) .

Contraction dynamics

The actual muscle part of the muscle model is modelled with a contractile element (CE), in series with a non-linear passive series-elastic element (SE). This chain is in parallel with a non-linear passive parallel-elastic element (PE). The CE is an active element in which force development is a function of the non-linear force-length and force-velocity relationships. In this part of the muscle model, activation a and muscle length L_m are input, and muscle force is output.

Force-length relation

To relate muscle length to fiber length, first the effects of pennation angle and tendon length must be taken into account:

$$d_0 = sin(\alpha_0) \cdot L_{CE,0}, \tag{A.4}$$

$$\alpha = asin(\frac{d_0}{L_{CE}}), \tag{A.5}$$

Where d_0 is the width of the muscle due to pennation. It is assumed that the muscle is bi-pennate (or multi-pennate) and that the width of the muscle does not change, i.e. d_0 is constant. α_0 is the initial pennation angle, and $L_{CE,0}$ is the optimum fiber length (optimum length CE). α is the actual pennation angle, and can be calculated from the actual fiber length L_{CE}. Hence, the length of the SE can be calculated:

$$L_{SE} = L_m - cos(\alpha) \cdot L_{CE} - L_t, \tag{A.6}$$

in which L_{SE} is the length of SE, L_m normalised muscle length and L_t the length of the tendon. L_{CE}, L_{SE} and L_t are all normalised with respect to optimum muscle length.

The normalised fore-length relation (or length-tension ratio lt_{rat}) can be described by a Gaussian curve:

$$lt_{rat} = cos(\alpha) \cdot e^{(\frac{L_{CE}-L_{CE,0}}{L_{cesh}})^2}, \tag{A.7}$$

where L_{cesh} is a shape parameter determining the width of the force-length relationship.

Series-elastic element

The force in the series-elastic element is a function of L_{SE}:

$$SE_{p1} = \frac{F_{max}}{e^{SE_{sh}-1}}, \tag{A.8}$$

$$SE_{p1} = e^{\frac{SE_{sh}}{SE_{xm}}}, \tag{A.9}$$

$$F_{SE} = SE_{p1} \cdot (SE_{p2}^{L_{SE}} - 1), \tag{A.10}$$

in which F_{max} is the maximal active muscle force derived from the PCSA, SE_{sh} is a shape parameter of the curvature of the exponential slope and SE_{xm} determines the maximal extension of the SE. F_{SE} is output of the contractile machinery of the muscle model.

Force-velocity relationship

The actual maximal contraction velocity of the muscle fiber is scaled by the force-length relation, and by the muscle activation:

$$v_{max} = MV_{vm}(1 - (MV_{er}(1 - lt_{rat} \cdot a))), \tag{A.11}$$

in which MV_{vm} is the initial maximal contraction velocity and MV_{er} is a scaling parameter. Then, for a concentric contraction ($rf < 1$):

$$v_{CE} = v_{max} \cdot MV_{sh} \cdot \frac{rf - 1}{rf + MV_{sh}}, \tag{A.12}$$

where v_{CE} is the contraction velocity of the contractile element, MV_{sh} is a shape parameter of the curvature of the force-velocity relationship. The force-velocity curve for lenghtening muscles has been obtained by inverting the force-velocity curve for shortening muscles:

$$v_{CE} = \frac{v_{max} \cdot MV_{shl} \cdot MV_{sh} \cdot (rf - 1)}{rf - 1 - (MV_{sh} \cdot MV_{shl} + 1) \cdot (MV_{ml} - 1)}, \tag{A.13}$$

where MV_{shl} is a shape parameter for the lengthening curve, and MV_{ml} is the maximal force for lengthening muscle. In order to prevent oscillations, the v_{ce} is constrained to be less than muscle velocity, and F_{se} is constrained to be less than MV_{ml}.

Parallel visco-elastic element

The force development in the parallel visco-elastic element is a function of the muscle length and the muscle velocity. The force-length relation is analogous with the SE:

$$PE_{p1} = \frac{F_{max}}{e^{(PE_{sh}-1)}}, \tag{A.14}$$

$$PE_{p2} = e^{\frac{PE_{sh}}{PE_{xm}}}, \tag{A.15}$$

$$F_{PE} = PE_{p1} \cdot (PE_{p2} \cdot 2^{(L_s - L_{PE,0})} - 1), \tag{A.16}$$

where PE_{sh} is a shape parameter, PE_{xm} is the maximal extension of the muscle and $L_{PE,0}$ the muscle rest length, i.e. the maximal length at which F_{PE} is zero.

The force-velocity relation is a simple linear relation:

$$F_{PV} = p_v \cdot v_m \cdot F_{max}, \tag{A.17}$$

where p_v is a constant and v_m is the normalised muscle velocity.

Total muscle force

the output of the muscle model is the total muscle force F_m:

$$F_m = F_{SE} + F_{PE} + F_{PV} \tag{A.18}$$

Parameter values

The following parameters are the same for all muscle elements in the DSEM:

SE_{sh}	=	3.00
MV_{vm}	=	-4.50
MV_{ml}	=	1.30
MV_{sh}	=	0.30
MV_{shl}	=	0.50
MV_{er}	=	0.50
PE_{sh}	=	4.00

Other parameters are muscle element specific and were based on cadaver measurements.

Appendix B. Problems with kinematics

For this study kinematic and EMG data were collected on four subjects following the test protocol in 2.2. Due to measurement errors which can be related to a lack of experience in this type of measurements, data for the first three test subjects could not be used. Both kinematic and EMG data were of good quality for the fourth subject. However, when running simulations with the DSEM (inverse mode, v4.2) errors occurred, leading to a model crash (ERROR 0: Check input kinematics). A description of the encountered problems and efforts that have been made in trying to solve these are presented in this appendix.

Appendix B.1. Translating subject to cadaver rotations

Thorax, scapula and clavicle form a closed-chain mechanism which is of great importance for estimating forces that act on the shoulder. To account for anatomical differences between cadaver and subject in the segments of this chain (i.e. differences in size of clavicle, scapula and thorax), a routine is included in the DSEM that translates scapular and clavicular rotations that were measured on a subject to cadaver rotations. This routine changes the measured scapular and clavicular angles to 'optimal' angles that close the chain on the cadaver and have minimal difference with the measured angles on the subject. In simulations with the DSEM optimised angles are used for calculating the position of the cadaver at a given timestep. To make sure the cadaver follows the measured motion, differences between measured and optimised angles may not become too large.

For subjects in other studies where the DSEM was used for, differences between measured and optimised angles in the order of 5° are found, but for this subject differences were much larger, namely up to 20° as can be seen in fig. B.8a. In the optimisation routine anterior tilt is lowered by 20° while scapular protraction is lowered by over 12° in the resting position (arm hanging vertically down). In fig. B.8b it can be seen that the scapula is put too superiorly on the thorax in an unrealistic position. This does not only show that the cadaver does not resemble the motion that is measured, but also leads to model crashes.

Because only two bony landmarks on the clavicle can be measured (SC and AC) the third rotation of the clavicle (axial rotation) is determined with a routine that minimises rotation in the AC-joint. With this routine a clavicular axial rotation of -100° is found while axial rotation in the anatomical position is supposed to be zero (by definition). Apparently, with the optimised angles as input, ligaments that attach scapula to clavicle have moment arms around the clavicular axis in other than the expected direction and force the clavicle in this 'flipped' position. The model can not assume this position and crashes.

Appendix B.2. Possible causes and solutions

Measured kinematics form the input to the DSEM. Measured segment rotations (bone rotations) are translated to cadaver segment rotation. The cadaver of an embalmed 57-year-old muscular man serves as a basis for the DSEM [2]. From these cadaver measurements a parameter file that includes muscle parameters, segment dimensions and inertia was built. Morphological differences between cadaver and subject introduces errors in DSEM predictions. When these differences become larger, accuracy of prediction decreases and, as was found in this study, can lead to model crashes. To find possible causes for the strange 'optimal' position of scapula and clavicle, the subject's anatomy was compared to the cadaver. Efforts have been made to make the cadaver look more like the subject by applying different scaling methods and changing the length of the conoid ligament.

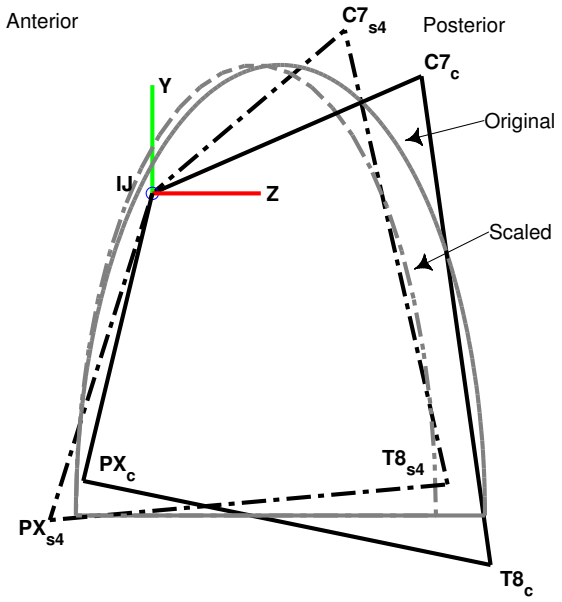

Figure B.9: Lateral view on the thorax with position of bony landmarks of the cadaver and test subject. IJ = Incisura Jugularis, PX = Processus Xiphoideus, C7 = Processus Spinosus of the 7th cervical vertebra, T8 = Processus Spinosus of the 8th thoracic vertebra. Subscript 'c' and 's' stand for cadaver and subject. The ellipsoid that represents the thorax shape of the cadaver before (solid) and after (dashed) scaling is drawn as well. The scaled thoracic wall fits better on the bony landmarks of the subject.

Appendix B.2.1. Scaling

Total body length of the cadaver could not be measured because the lower body half had been removed before it came available but was estimated to be 168 cm. The subject is tall (191 cm) and is of athletic build. To account for this difference, uniform scaling was applied. In all directions the cadaver was resized by a scale factor that was based on difference in total body length: $191cm/168cm = 1.14$. However, this did not have the desired effect: difference between optimised and measured angles was still large and no feasible position was found for the clavicle, leading to a model crash. Other scale factors

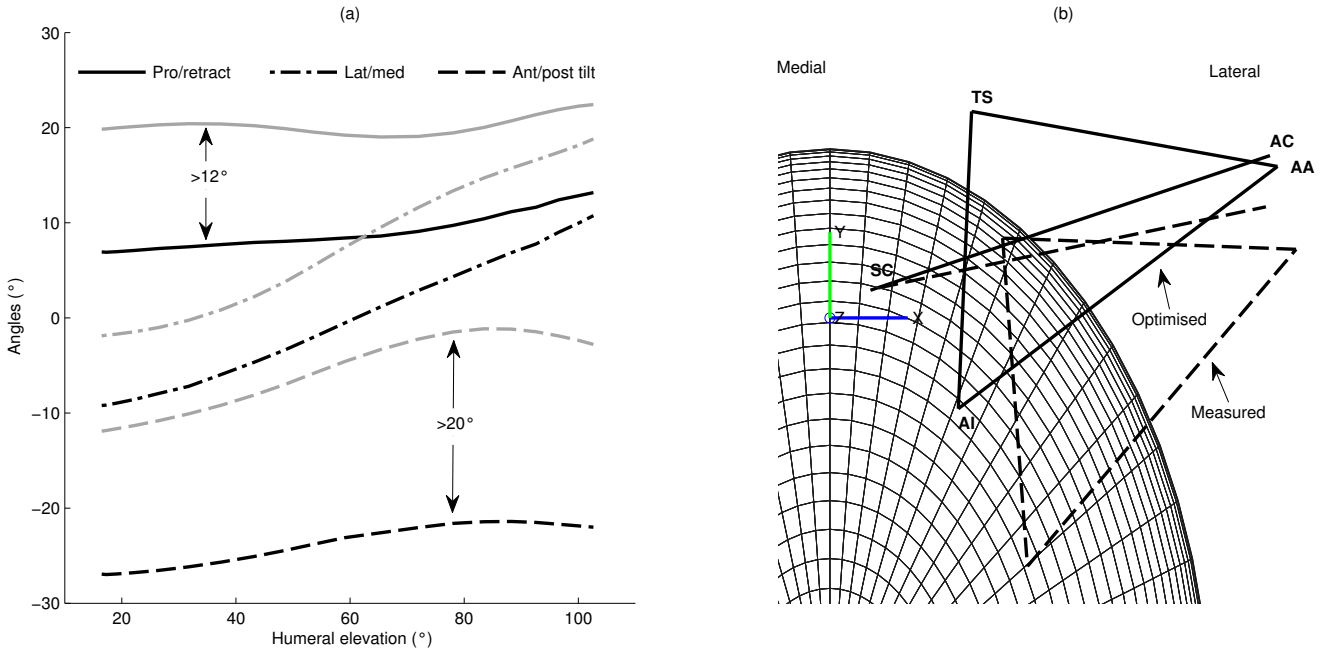

Figure B.8: a) Measured (grey) and optimised (black) angular rotations of the scapula for an abduction movement. Reasonable differences would be in the order of 5°, but on the subject differences were found to be even larger than 20°. b) Dorsal view of the thorax with measured (dashed) and optimised (solid) initial position of the right scapula (represented by the lines connecting Trigonum Spinae (TS), Angulus Inferior (AI) and Angulus Acromialis (AA)) and clavicle (the line connecting the sternoclavicular joint (SC) and acromioclavicular joint (AC)). An unrealistic position is calculated in the optimisation routine where the scapula is put extremely high on the thorax (low protraction and high anterior tilt). This causes problems when running simulations with the DSEM.

based on eg. difference in armlength were tried as well, but none of them solved the problems.

No joint is present between thorax and scapula, but this does not mean that the scapula can move independently from the thorax. The connection between scapula and thoracic wall is formed by the scapulothoracic gliding plane. Mathematically, this connection is described in the kinematic optimisation routine (see Appendix B.1) by constraining the scapula to be on a fixed distance of approximately 2cm to the ellipsoid that represents the thoracic wall. Becasue of this constraint, the shape of the ellipsoid is important in the kinematic optimisation routine.

Most remarkable about the anatomy of this subject is the relatively small size of the thorax in the anterior-posterior direction ('flat' thorax). This difference in thorax shape was also reflected in positions of bony landmarks on the thorax as can be seen in fig B.9). The thoracic wall in the DSEM is represented by an ellipsoid that was fitted on bony landmarks on the cadaver's thorax. These bony landmarks of the subject fall inside this ellipsoid. The flat thorax of this subject is also reflected in low scapular protraction in the resting position: 15° in the subject, while 25° was measured on the cadaver.

In a second attempt to solve the kinematic problems, parameters that describe the thoracic ellipsoid were changed so that it showed more similarity with the bony landmarks that were measured on the subject. Because dissimilarities between cadaver and subject were mainly in the anterior-posterior (z-)direction, the thorax was nonuniformly scaled: only z-values for ellipsoid centre and axes were changed, in the x- and y-direction the values were kept the same. The scale factor was chosen so that the distance between the midpoint of C7-T8 of the cadaver and the original ellipsoid was the same as the distance between midpoint C7-T8 of the subject and the scaled ellipsoid and was found to be 0.88. The centre was slightly shifted in the z-direction (anteriorly) so that on the anterior side the scaled ellipsoid coincides with the original[3] (see fig. B.9).

With this scaled thorax, optimised clavicular and scapular motion followed measured motion better. Scapular protraction which was lowered by 12° with the original cadaver file (B.8a) was now lowered by 8°. In the other optimised angles the effect of non-uniform scaling was even more pronounced: anterior tilt which was increased by 20° with the original cadaver file now only showed a difference of 3° in the resting position. This indicates that the optimal position of the thorax was not too superiorly

[3]When the thorax is nonuniformly scaled, attachment sites of thoracic muscles can go inside the thorax, causing problems when doing simulations with the DSEM (error code: KROMELL). As a solution to this, the attachment sites of these muscles were shifted in the z-direction to a position where they had same distance to the scaled ellipsoid as they had with the original ellipsoid.

on the thorax anymore but in a more realistic position on the dorsal side.

Although nonuniform scaling resulted in better correspondence between measured and optimised angles and scapula and clavicle were not moved to an (at first sight) unrealistic position, the model still crashed when recalculating axial rotation of the clavicle.

Appendix B.2.2. Conoid length

Because the cause of the problem could no longer only be subscribed to anatomical differences in thoracic shape, in a next step in trying to find a solution the connection between scapula and clavicula was further investigated. An important part of this connection is formed by the conoid ligament. On the cadaver conoid length was measured to be 1.18cm, which is short compared to lengths measured on other cadavers [10]. Apparently, in earlier simulations with the DSEM the short measured conoid length gave problems, because in the default DSEM the ligament is lengthened by 0.76cm to make it closer to lengths measured on other cadavers. Now problems arose in finding a feasible position and force equilibrium for the clavicle, the effect of changing the conoid length was looked at again.

Step by step the conoid was further lengthened. Changing conoid length also has effect in the kinematic optimisation routine for scapula and clavicle. Increasing the conoid length further increased differences between measured and optimised angles and problems in positioning the clavicle were not solved. Decreasing conoid length showed better results: with the conoid set at the length as was measured on the cadaver (1.18cm) all angles in the optimisation were changed with less than 5° which can be assumed to be reasonable. Moreover, force equilibrium was found for the clavicle and no 'flipped' clavicle was found anymore[4].

The physical interpretation of this model adaptation is hard to justify when looking at measured lengths of conoid ligaments. A conoid ligament length of 1.18cm is well outside the range of measured lengths on other cadavers [10]. Measurements errors or changes in length during the embalming process might have caused this. However, since shortening the conoid to its measured length (which was assumed to be unrealistic) had the desired effect it can be argued that the (short) measured conoid ligament was in fact exceptional, but correct. Rare connections between scapula and clavicle have been reported more often: in some cases even the presence of an articular connection (coracoclavicular joint) was found [8]. After this early study, more cases have been reported. Studies performed on a Korean [5] and northwest Indian population [14] both found an incidence of 10%. The presence of a coracoclavicular joint in the subject might be an explanation for the short conoid length. However, when this joint would be present, the kinematic chain would change, leading to different kinematics and force balances that can not be accounted for by the DSEM.

Other explanations might be found in other morphological differences between cadaver and the subject, eg. attachment sites of the conoid on the clavicle and/or scapula or lengths of other ligaments. Although no clear explanation can be given for the short conoid, the model does not give errors and muscle prediction seems to be feasible for both movements that were measured (anteflexion and abduction). It was therefore chosen to use a conoid length of 1.18cm and the non-uniformly scaled thorax for the simulations.

[4] In the initial step some problems occur in finding force equilibrium on the clavicle (error code: ARRFCLA) , but the DSEM finds a way to work around this by resetting the position of some nodes in the routine 'resetbones.f'

Appendix C. How to use DSEM in EMG and IFDO-mode

This appendix is intended for DSEM users who want to use the inverse model in IFDO- and EMG-mode. The *DSEM User's Guide* gives a general description of how to use the inverse DSEM and can be found in the docs-folder of the DSEM-v4.2-package, so here only the additional things that should be done are described.

Appendix C.1. IFDO-mode

To run the inverse DSEM in IFDO-mode the option `-ifdo` is added to the command line. The following command reads in *file.input* and runs the inverse DSEM in IFDO-mode:

`inverse -ifdo <`*file.input*

Appendix C.2. EMG-assisted mode

To run the EMG-assisted mode of the DSEM 3 things should be done:

1. An EMG file with extension *.emg* should be created.
2. The option `-emg1` or `-emg2` should be added to the command line.
3. 5 lines should be added to the end of the input-file.

1. EMG file

The EMG file contains a matrix M of size $nsteps \times n$ with $nsteps$ the number of steps in the sample (should be equal to number of samples in the motion file) and n the number of EMG signals, in which each value $M_{i,j}$ is a number between 0 and 1 representing filtered EMG (normalised to maximum value) in step i for muscle j. In other words, each column in the EMG file represents a processed EMG-signal.

2. Command line options

Two EMG-assisted modes of the DSEM, called the EMG1 and EMG2-mode, are available. Both modes constrain the inverse optimisation by setting excitation equal to measured EMG for some muscles (see 2.1.4 for a more elaborate description). The two modes differ in the way boundaries for muscle elements where EMG is not measured from (or is not switched on for) are defined.

- In mode EMG1 these bounds are defined as in the IFDO-mode: $F_{min} \leq F_{mus} \leq F_{max}$ where F_{min} and F_{max} are calculated in a forward muscle model with hypothetical neural input of respectively 0 and 1.
- In mode EMG2 these bounds are defined as in the IDO-mode: $0 \leq F_{mus} \leq F_{rel,max} \cdot PCSA \cdot \sigma_{max}$.

By adding option `-emg1` or `-emg2` to the command line the inverse DSEM is run in the EMG1- respectively EMG2-mode.

3. Changes in input-file

The input-file should look like this.

```
'../output/output_file'
'header'
'mode'
'filter.par' *** only for 'dyn' mode ***
'../input/motion_file.inp'
a b c d
'y/n'
input option
'parameter file code'
'../dasp/parameter_file.dsp'
'../dasp/parameter_file.num'
'../dasp/parameter_file.spc'
cost
'../input/emg_file.emg'
n
f1,f2,fi,...,fn
l1,l2,li,...,ln
s1,s2,si,...,sn
```

Only the last 5 lines are added (compared to the input-file for the normal inverse mode), so only the meaning of these lines will be described here. The other input arguments can be looked up in the *DSEM User's Guide*.

EMG file is the file location of the EMG file;

n represents the number of columns (EMG channels) in the EMG-file;

f is a row of n integers of which number f_i represents the first muscle element the EMG-value in column i of the EMG-file is assigned to;

l is a row of n integers of which number f_i represents the last muscle element the EMG-value in column i of the EMG-file is assigned to;

s is a row of n integers of which each number s_i is either '0' or '1'. If $s_i = 1$, EMG in column i of the EMG file is set equal to excitation for muscle elements f_i to l_i. If $s_i = 0$, EMG in column i is not used.

To clarify this, an example will be given.

Example:
EMG was measured for 6 muscles:

1. M. Pectoralis Major - thoracic part
2. M. Deltoideus - anterior part
3. M. Deltoideus - medial part
4. M. Deltoideus - posterior part
5. M. Infraspinatus
6. M. Trapezius - clavicular part

First, EMG should be filtered, normalised to maximum values and resampled so the EMG signal is of equal length to the motion file. Processed EMG for muscle j is written to column j in the file *sample.emg*. This file is saved in the subfolder *../input* in the DSEM-folder.

The following 5 lines are added to the input-file:

```
'../input/sample.emg'
6
 139 91  85  80  44  55
 144 94  88  84  54  56
   1  0   1   0   0   0
```

The first line contains the file-location of the EMG file, the second line the number of columns in the EMG file. The first number of line 3 and 4 (139 and 144) assign EMG in column 1 of the EMG file to muscle elements 139-144 (representing M. Pectoralis major - thor. part). Similarly, the second number of line 3 and 4 (91 and 94) assign EMG in column 2 of the EMG file to musce elements 91 to 94, etc. The numbering of muscle elements can be found in table C.4.

The last line determines whether EMG for muscle j is switched on (1) or off (0). If EMG is switched off, EMG in the corresponding column is not used to constrain the inverse optimisation. In this example only column 1 and 3 are switched on, meaning that EMG in column 1 is set equal to excitation of muscle elements 139-144 and EMG in column 3 to muscle elements 85-88. EMG for other muscle elements can be switched on by changing the 0's in the last line to 1's. Assigning the EMG to other muscle elements can be done by changing the numbers in line 3 and 4.

Finally, the EMG-assisted mode is run by running the following command in the DOS-prompt in the folder that contains the file *inverse.exe*:

```
inverse -emg1 <sample.input
```

Table C.4: Most muscles are subdivided in multiple elements. In this table it can be looked up what muscle elements belong to what muscle. F stands for the first element number in the muscles, L for the last element number.

#	Muscle	F	L
1	M. Trapezius, scap. part	44	54
2	M. Trapezius, clav. part	55	56
3	M. Levator scapulae	57	58
4	M. Pectoralis minor	59	62
5	M. Rhomboideus	63	67
6	M. Serratus anterior	68	79
7	M. Deltoideus, scap. part	80	90
8	M. Deltoideus, clav. part	91	94
9	M. Coracobrachialis	95	97
10	M. Infraspinatus	98	103
11	M. Teres minor	104	106
12	M. Teres major	107	110
13	M. Supraspinatus	111	114
14	M. Subscapularis	115	125
15	M. Biceps, caput longum	126	126
16	M. Biceps, caput breve	127	128
17	M. Triceps, caput longum	129	132
18	M. Latissimus dorsi	133	138
19	M. Pect. major, thor. part	139	144
20	M. Pect. major, clav. part	145	146
21	M. Biceps, cap. long. elbow	147	147
22	M. Triceps, medial part	148	152
23	M. Brachialis	153	159
24	M. Brachioradialis	160	162
25	M. Pronator teres, hum-rad	163	163
26	M. Pronator teres, uln-rad	164	164
27	M. Supinator, hum-rad	0	0
28	M. Supinator, uln-rad	165	169
29	M. Pronator quadratus	170	172
30	M. Triceps, lateral part	173	177
31	M. Anconeus	178	182